Inhibiting PI3K reduces mammary tumor growth and induces hyperglycemia in a mouse model of insulin resistance and hyperinsulinemia

Emily Jane Gallagher, MB BCh BAO, MRCPI[*], **Yvonne Fierz, MD**[*], **Archana Vijayakumar, B. Tech**, **Nadine Haddad, MD**, **Shoshana Yakar, PhD**, and **Derek LeRoith, MD PhD**
Division of Endocrinology, Diabetes and Bone Disease, Mount Sinai School of Medicine, Box 1055, New York, NY 10029, USA

Abstract

Women with type 2 diabetes (T2DM) are at greater risk of developing and dying from breast cancer than women without T2DM. Insulin resistance and hyperinsulinemia underlie the pathogenesis of T2DM. In the MKR mouse model of insulin resistance, we have previously shown increased activation of the phosphatidylinositol 3-kinase (PI3K)/Akt/mTOR pathway in association with accelerated mammary tumor growth. In this study, we demonstrate that inhibiting PI3K with the oral pan-class I PI3K inhibitor, NVP-BKM120 reduced the growth of Met-1 and MCNeuA mammary tumor orthografts in the MKR mouse. NVP-BKM120 treatment decreased phosphorylation of Akt and S6 ribosomal protein (S6rp); no change in Erk1/2 phosphorylation was seen. Hyperglycemia, hypertriglyceridemia and greater hyperinsulinemia developed in the MKR mice treated with NVP-BKM120. We previously reported reduced tumor growth using intraperitoneal rapamycin in the MKR mouse, with the development of hyperglycemia and hypertriglyceridemia. Therefore, we examined whether the oral PI3K/mTOR inhibitor NVP-BEZ235 augmented the tumor suppressing effects of PI3K inhibition. We also investigated the effect of targeted PI3K/mTOR inhibition on PI3K/Akt/mTOR and Erk1/2 signaling, and the potential effects on glycemia. NVP-BEZ235 suppressed the growth of Met-1 and MCNeuA tumor orthografts, and decreased Akt and S6rp phosphorylation, despite increased Erk1/2 phosphorylation in Met-1 orthografts of MKR mice. Less marked hyperglycemia and hyperinsulinemia developed with NVP-BEZ235 than NVP-BKM120. Overall, the results of this study demonstrated that inhibiting PI3K/Akt/mTOR signaling with the oral agents NVP-BKM120 and NVP-BEZ235 decreased mammary tumor growth in the hyperinsulinemic MKR mouse. Inhibiting PI3K alone led to more severe metabolic derangement than inhibiting both PI3K and mTOR. Therefore, PI3K may be an important target for the treatment of breast cancer in women with insulin resistance. Monitoring for hyperglycemia and dyslipidemia should be considered when using these agents in humans, given the metabolic changes detected in this study.

Corresponding Author: Derek LeRoith, Division of Endocrinology, Diabetes and Bone Disease, Mount Sinai School of Medicine, Box 1055, One Gustave L. Levy Place, New York, NY 10029, Derek.LeRoith@mssm.edu, Tel: 212-241-1500, Fax: 212-241-4218.
[*]Authors EJG and YF contributed equally to the work in this manuscript

Keywords

Insulin resistance; diabetes; breast cancer; PI3K inhibitor

Introduction

Women with type 2 diabetes mellitus (T2DM) and the metabolic syndrome (a syndrome of insulin resistance and hyperinsulinemia) are at greater risk of developing and dying from breast cancer than women without these conditions (Patterson 2010, Agnoli 2010, Peairs 2011). Even in the absence of T2DM or the metabolic syndrome, having a fasting insulin level that lies in the upper quartile of the normal population range has been reported to increase the risk of breast cancer recurrence and death, in women with early stage breast cancer (Goodwin 2002). In human breast cancer, insulin receptor (IR) content is frequently increased (Papa 1990) and therefore, in the setting of insulin resistance and hyperinsulinemia, activation of the IR and its downstream signaling pathways may promote breast cancer growth. In our previous studies, we have employed the female MKR mouse to investigate the mechanisms underlying the link between hyperinsulinemia and breast cancer. The female MKR mouse has significant insulin resistance and hyperinsulinemia with mild glucose intolerance (Novosyadlyy 2010). Our previous studies have demonstrated that female MKR mice develop larger mammary tumors, than wild type (WT) mice. The IR/ insulin like growth factor-1 receptor (IGF-1R)/phosphatidylinositol 3-kinase (PI3K)/Akt/ mTOR pathway was the main signaling pathway that demonstrated increased activation in tumors from the MKR mice (Novosyadlyy 2010).

The PI3K/Akt/mTOR signaling pathway and its activation by IRβ / IGF-IRβ phosphorylation has recently received intense investigation, with the emergence of resistance to current chemotherapeutic agents and the identification of mutations that lead to dysregulation of this pathway (Junttila 2009, Lopez-Knowles 2010, Creighton 2010). PI3K consists of 2 subunits, a p110 catalytic subunit and its regulatory p85 subunit. After receptor phosphorylation, binding of adaptor proteins, such as insulin receptor substrate-1 (IRS-1), to the p85 subunit releases the p110 catalytic subunit from its inhibitory regulation and allows for the phosphorylation of phosphatidylinositol-4,5-bisphosphate (PIP_2) to generate phosphatidylinositol-3,4,5-triphosphate (PIP_3). PIP_3 phosphorylates Akt leading to the activation of a plethora of signaling molecules. Multiple gene mutations can increase signaling through the PI3K/Akt/mTOR pathway in breast cancers, for example loss of activity of the tumor suppressor gene phosphatase and tensin homologue deleted on chromosome ten (PTEN), amino acid substitutions in PI3KCA (encoding the p110α catalytic subunit of PI3K), overexpression of human epidermal growth factor receptor-2 (HER-2) and mutations in Akt. In cell lines, increased PI3K signaling has been shown to confer resistance to the monoclonal antibody trastuzumab that is directed against HER-2 and is used to treat HER-2 receptor positive breast cancers in women (O'Brien NA 2010). Additionally, in estrogen receptor (ER) positive breast cancer cells, PI3K activity is associated with decreased expression of ER and ER target genes. This decreased ER expression in ER positive tumors is associated with resistance to hormonal therapy (Creighton 2010). Therefore, insulin resistance and endogenous hyperinsulinemia, leading to

increased activation of the PI3K signaling pathway, may result in resistance to HER-2 and ER targeted therapy and so may be an important therapeutic target in individuals with breast cancer who have increased insulin levels, the metabolic syndrome or T2DM.

However, two particular concerns have arisen with regard to inhibiting the PI3K/Akt/mTOR pathway. Firstly, that inhibition of PI3K signaling in HER-2 overexpressing tumors will lead to a compensatory increase in Erk1/2 signaling, as was recently described with the PI3K inhibitors, GDC-0941 and PIK-90 in cell lines and the dual PI3K/mTOR inhibitor, BEZ235 in xenografts inoculated into mice (Serra 2011). The second concern is that inhibiting PI3K may result in significant hyperglycemia. We have previously demonstrated that inhibiting mTOR with rapamycin led to increased glucose and triglyceride levels in MKR mice, but did not lead to a further increase in the already elevated plasma insulin levels and did not affect Ser^{473} phosphorylation of Akt in tumors (Fierz 2010). PI3K inhibition would be expected to lead to different metabolic effects than rapamycin, due to the effects of PI3K inhibition on the phosphorylation of Akt and on atypical isoforms of protein kinase C (PKC)ζ. Both Akt and atypical isoforms of PKCζ are important for insulin mediated glucose uptake in muscle and adipose tissue by glucose transporter 4 (GLUT4) (Kohn 1996, Liu 2006).

Therefore, we aimed to examine the effect of inhibiting PI3K on tumor progression and metabolic parameters, in a mouse model of hyperinsulinemia. In this study we inhibited PI3K with the oral pan-class I inhibitor of PI3K, NVP-BKM120 and evaluated the growth of mammary tumor orthografts in the hyperinsulinemic MKR mouse. We examined the PI3K/Akt/mTOR signaling pathway to determine whether this inhibitor could adequately block signaling in tumors from the MKR mouse, where the activity of this pathway is known to be increased. We also studied the phosphorylation of Erk1/2 to determine whether inhibition of PI3K led to a compensatory increase in Erk1/2 signaling in the MKR mouse. Additionally, we examined the effects of inhibiting PI3K on metabolic parameters, including glucose, insulin and triglyceride levels. Finally, in view of our previous study demonstrating that inhibiting mTOR with rapamycin led to hyperglycemia in the MKR mouse, but reduced tumor growth (Fierz 2010), we were interested to know if inhibiting both PI3K and mTOR with the targeted dual inhibitor, NVP-BEZ235 would lead to an additional suppression of tumor growth and if it would affect insulin and glucose levels in the MKR mouse. We also aimed to discover whether the dual PI3K/mTOR inhibitor would lead to a compensatory increase in Erk1/2 signaling in this model, similar to the results from animal models without insulin resistance (Serra 2011).

Results

Inhibiting PI3K reduces tumor growth in the MKR mouse

The MKR mouse is a nonobese animal model of type 2 diabetes. The female MKR mouse has marked hyperinsulinemia, but only mild dysglycemia. We have previously demonstrated that after orthotopic inoculation of Met-1 and MCNeuA cells into the 4th mammary fat pad, MKR mice develop larger tumors than wild-type (WT) mice (Novosyadlyy 2010). Met-1 mammary tumor cells were initially derived from MMTV-Polyoma Virus middle T antigen (PyVmT) transgenic mice (Borowsky *et al.* 2005) and MCNeuA mammary tumor cells were

derived from MMTV-Neu transgenic mice, the rodent equivalent of the human ErbB2 or HER-2 gene (Campbell *et al.* 2002). Met-1 cells have a high proliferation rate and have a mesenchymal phenotype. MCNeuA cells have an epithelial phenotype and have a low proliferation rate.

We orthotopically inoculated MKR mice and WT mice with Met-1 and MCNeuA cells, as previously described (Novosyadlyy 2010). Cells were injected one week apart, to allow for the lower proliferation rate of the MCNeuA cells. 2 weeks after injection of the Met-1 cells and 3 weeks after injection of MCNeuA cells, the MKR and WT mice were divided into 2 treatment groups that were matched for respective tumor size (Figure 1A and 1C). Mice were treated with NVP-BKM120 (50mg/kg) by oral gavage, or the same volume of the vehicle. Treatment continued for 2 weeks with interval measurement of tumor growth over that time and measurement of tumor weight at the end of the study. The volumes of both Met-1 and MCNeuA tumors were significantly lower in the MKR mice treated with NVP-BKM120, compared to the MKR vehicle treated group (Figure 1A and 1C). Similarly, the weights of MCNeuA and Met-1 tumors were significantly reduced in the MKR group treated with NVP-BKM120 and the MCNeuA tumor weights were also significantly reduced in the WT group (Figure 1B and 1D). Therefore, in the insulin resistant, hyperinsulinemic mouse, inhibiting PI3K with NVP-BKM120 decreases the growth of mammary tumors known to have increased activation of the PI3K/Akt/mTOR signaling pathway.

Blocking PI3K signaling with NVP-BKM120 reduces tumor growth by inhibition of Akt signaling in the MKR mouse

Our previous studies have demonstrated an increase in phosphorylation of $IR\beta^{(Tyr1150/1151)}$ / $IGF\text{-}IR\beta^{(Tyr1135/1136)}$ and $Akt^{(Ser473)}$ in Met-1 and MCNeuA tumors inoculated into MKR mice, compared to those injected into WT FVB/N mice (Novosyadlyy 2010). No change was seen in phosphorylation of $Akt^{(Ser473)}$ in response to treatment with the mTOR inhibitor rapamycin (Fierz 2010). In this study, we again observed a statistically significant increase in $Akt^{(Ser473)}$ phosphorylation in the MKR vehicle treated group compared to the WT vehicle treated groups (Figure 2A, 2B, this difference is not marked with an asterisk on the densitometry 2C and 2E). Inhibiting PI3K resulted in decreased phosphorylation of $Akt^{(Ser473)}$ in both WT and MKR mice, along with decreased phosphorylation of S6 ribosomal protein$^{(Ser235/236)}$ (Figure 2A–2F). No change in $Erk1/2^{(Thr202/204)}$ phosphorylation was seen in either WT or MKR mice treated with NVP-BKM120 (Figure 2 G–J). Overall, NVP-BKM120 successfully reduces phosphorylation of Akt and S6 ribosomal protein in tumors from the MKR mouse that is known to have increased activation of Akt signaling.. No change in Erk1/2 signaling was seen after treatment with NVP-BKM120 in either cell type in MKR or WT mice.

Inhibiting PI3K led to reduced proliferation in Met-1 tumor orthografts in MKR mice

We have previously demonstrated increased proliferation in the Met-1 tumors in MKR mice by evaluation of protein extracts for proliferating cell nuclear antigen (PCNA) on western blot (Fierz 2010). To examine whether this increase in S phase growth was inhibited with NVP-BKM120, the mice were injected with 5-bromo-2'-deoxyuridine (BrdU) 2 hours prior to tumor tissue collection. The percent of cells that stained positive for BrdU in the Met-1

tumors was evaluated by immunofluorescence. We found a significantly higher percent of BrdU positive cells in the vehicle treated MKR mice (9.9 ±0.76%), compared to vehicle treated WT mice (7.8±0.35%) (Figure 3A). Treatment of the MKR mice with NVP-BKM120 led to a significantly lower percent of BrdU positive cells (5.8±1.13%), compared to vehicle treated MKR mice (P=0.001). The percent of BrdU positive cells in the Met-1 tumors from the MKR mice treated with NVP-BKM120 was comparable to the percent of BrdU positive cells in the WT NVP-BKM120 treated group (5.8±0.63%). Therefore, in the MKR mice, inhibiting PI3K with NVP-BKM120 attenuated the increased cellular proliferation in Met-1 tumors from the MKR mice (Figure 3B). Western blot analysis of apoptosis, using the antibody to the anti-apoptotic protein Bcl-2 revealed decreased levels of Bcl-2 when normalized to β actin, in the MKR vehicle treated group, compared to the MKR NVP-BKM120 treated group (data not shown).

Mice treated with NVP-BKM120 developed metabolic derangements

Before treatment, MKR mice had mildly elevated blood glucose levels (10.6 ±0.5 mmol/L), compared to WT mice (7.2 ± 0.2 mmol/L) (Figure 4A). Following 2 weeks of treatment, significant hyperglycemia developed in the WT and MKR groups treated with NVP-BKM120 (Figure 4), and was demonstrated during the glucose tolerance test (Figure 4B). Plasma insulin levels revealed that WT and MKR mice treated with NVP-BKM120 had significant hyperinsulinemia, compared to the vehicle treated mice, with the levels for the WT mice increasing ~7 fold and for MKR mice rising more than 10 fold (Figure 4C). Triglyceride levels also increased in the MKR mice treated with NVP-BKM120 to a modest (1.5 fold increase) but significant degree, although no increase was seen in the WT mice (Figure 4D).

Comparison of PI3K inhibition alone with the PI3K and mTOR dual inhibitor NVP-BEZ235

We were interested to discover the effects of inhibiting both PI3K and mTOR on the tumor growth and glucose control in the MKR mice. Our previous studies had demonstrated that the mTOR inhibitor rapamycin reduced tumor growth, but increased glucose levels in the MKR mice, while our current study demonstrated that inhibiting PI3K with NVP-BKM120 also reduced tumor growth, but led to more severe hyperglycemia and hyperinsulinemia than rapamycin. We therefore speculated that inhibiting both PI3K and mTOR could have a synergistic effect on the reduction in tumor growth. Analogous to the study with NVP-BKM120, we inoculated the 4th mammary fat pad of WT and MKR mice with Met-1 and MCNeuA cells, and divided them into treatment groups, with the dual PI3K / mTOR inhibitor NVP-BEZ235 (40mg tosylate salt/ kg body weight) or the vehicle (10% NMP: 90% PEG300), by daily gavage for 2 weeks. Before treatment began, the groups were matched for tumor size, and serial measurements were taken during the study to calculate the tumor volume. At the end of the study tumor weights were also recorded. Proteins from the MCNeuA and Met-1 tumors were isolated, as previously described and again phosphorylation of the Akt, S6 ribosomal protein and Erk1/2 were examined relative to their total protein levels.

The volumes of both MCNeuA and Met-1 tumors were again significantly decreased in the MKR mice treated with the dual PI3K / mTOR inhibitor NVP-BEZ235 (Figure 5A, 5B),

tumor weight was not significantly different in the treatment groups as there was a wide distribution in the tumor weights due to variable areas of necrosis (Figure 5C, 5D). Analysis of tumor proteins revealed a significant decrease in phosphorylation of Akt and S6 ribosomal protein in the MKR and WT NVP-BEZ235 treated group, compared with the vehicle treated groups (Fig 5E, 5F, 5G, 5I). In contrast to the PI3K inhibitor NVP-BKM120, an increase Erk1/2 phosphorylation was seen in the Met-1 tumors from MKR mice treated with NVP-BEZ235, when compared to those treated with the vehicle (Figure 5J). Glucose intolerance and hyperinsulinemia developed in the MKR mice treated with NVP-BEZ235 (Figure 6A, 6B), but the degree of glucose intolerance and hyperinsulinemia was not as great as with NVP-BKM120 treatment. No significant hyperinsulinemia developed in the WT group treated with NVP-BEZ235, compared to controls (Figure 6B).

Discussion

Our results demonstrate that in the MKR mouse model of insulin resistance, inhibiting PI3K with NVP-BKM120 decreased the growth of tumor orthografts known to have increased activation of the PI3K/Akt/mTOR pathway in the hyperinsulinemic mouse. In the MKR mouse, inhibiting PI3K alone reduced Akt phosphorylation and did not lead to a compensatory increase in Erk1/2 signaling. In contrast to our study of rapamycin, inhibiting both PI3K and mTOR led to a reduction in Akt phosphorylation as well as a decrease in S6rp phosphorylation, however increased activation of Erk1/2 signaling in Met-1 tumors from the MKR mouse treated with NVP-BEZ235 was seen. These results are partially consistent with the findings of other groups, who reported that inhibition of PI3K alone (with GDC-0941 and PIK90), or in combination with mTOR (NVP-BEZ235) led to a compensatory increase in Erk1/2 signaling in tumor xenografts (Serra 2011). Notably, the PI3K inhibitors used were different as were the cell lines and animal models, all of which could account for the different findings regarding Erk1/2 phosphorylation.

Other studies, in addition to ours, have reported that inhibiting PI3K results in no change, or in some cases, a reduction in Erk1/2 signaling (Wells 2007). As well as differences in cellular characteristics, different pharmacological agents possess varying activity against the different class 1A p110 isoforms of PI3K. Although in breast cancer, the PI3KCA gene that encodes for the p110α, is the most commonly mutated of the 3 class 1A isoforms (p110α, p110β, p110δ), evidence from other cell lines show that inhibiting 2 of these 3 isoforms is insufficient to inhibit cell proliferation and survival (Foukas 2010). Therefore, PI3K inhibitors that preferentially target p110α (GDC-0941 and PIK90), may not be as effective at preventing cellular proliferation and cell cycle progression, as pan class 1A inhibitors such as NVP-BKM120 and XL147.

The more pronounced glucose and insulin derangements in the WT and MKR mice treated with the PI3K inhibitor NVP-BKM120, may be the result of more pronounced PI3K and Akt inhibition with this compound than with the dual PI3K/mTOR inhibitor NVP-BEZ235. Our protein analysis demonstrated that the inhibition of Akt phosphorylation with NVP-BEZ235 was less marked than with the PI3K inhibitor NVP-BKM120. Similar findings regarding Akt phosphorylation have previously been reported, and other studies have demonstrated an increase in Akt phosphorylation at lower doses of NVP-BEZ235 (Serra 2008, Serra 2011).

At low concentrations, NVP-BEZ235 predominantly inhibits mTORC1 activity, while at higher concentrations it inhibits PI3K and mTORC1/2. Therefore, in our study, the disproportionately greater suppression of S6 ribosomal protein phosphorylation, compared to Akt phosphorylation in NVP-BEZ235 treated tumors, may be the result of the different inhibitory concentration of NVP-BEZ235 on mTOR and Akt.

Insulin signaling is important for glucose uptake into skeletal muscle and adipose tissue, by the glucose transporter GLUT4. Previous studies have demonstrated that inhibiting PI3K with wortmannin and LY294002 prevents the translocation of GLUT4 to the cell surface and glucose uptake into cells. Akt and atypical PKCζ are important downstream targets of PI3K that mediate this glucose uptake (Liu 2006). Inhibitors of Akt have also been reported to cause hyperglycemia, by GLUT4 dependent and independent mechanisms (Tan 2010). Only very low levels of Akt appear to be necessary to maintain GLUT4 function in certain cells, suggesting alternative unknown mechanisms are also in play (Tan 2010). The difference in Akt inhibition between with NVP-BKM120 compared to NVP- BEZ235 may partly explain the more dramatic hyperglycemia that was observed with NVP-BKM120. Some studies using PI3K inhibitors have not reported dramatic hyperglycemia, an affect that may be related to the p110 isoform of PI3K that is inhibited: a pan class IA inhibitor may lead to more severe glucose derangement than a selective p110α inhibitor, although the roles that the different p110 isoforms play in the metabolic effects of insulin remain to be determined (Sopasakis 2010, Jia 2008).

In addition to more severe hyperglycemia, we noted more dramatic hyperinsulinemia with the PI3K inhibitor compared with the dual PI3K/ mTOR inhibitor, which caused greater hyperinsulinemia than rapamycin (Fierz 2010). Inhibition of PI3K and Akt will directly lead to insulin resistance by preventing signal transduction through this pathway. Inhibiting mTOR in addition to PI3K may in fact improve insulin sensitivity, as the mTOR/S6 Kinase pathway causes serine phosphorylation of IRS-1, which attenuates signaling. Therefore, inhibiting mTOR/S6 Kinase activity may reduce some of the insulin resistance caused by PI3K inhibition, by relieving the inhibition of serine phosphosylation of IRS-1 and allowing tyrosine phosphorylation of IRS-1 and activation of the insulin signaling pathway (Um 2006).

In conclusion, our study demonstrates that PI3K inhibitors reduce tumor growth in an animal model of insulin resistance and hyperinsulinemia. These results may be particularly relevant in individuals with insulin resistance, the metabolic syndrome and T2DM, who may have dysregulation of the PI3K pathway in breast cancer, as demonstrated in our mouse model. In our model, we demonstrate that with pan class 1 PI3K inhibition, there is no increase in activation of Erk1/2 signaling. Our data demonstrates a similar reduction in tumor growth with the dual PI3K/mTOR inhibitor and PI3K inhibition alone. However, dual inhibition of PI3K and mTOR importantly led to less severe hyperglycemia and hyperinsulinemia, which may be due to either less potent inhibition of Akt by NVP-BEZ235 or due to a reduction in insulin resistance by inhibiting mTOR. Based on the results of our study and other similar studies, many questions regarding the role of PI3K in tumor growth and metabolism have emerged. Future studies are needed to address the roles of hyperinsulinemia and diabetes in breast cancer mortality in women (Peairs 2010).

Understanding more about the specific p110 isoforms in tumor growth and metabolism is necessary so that targeted therapy can lead to maximal tumor inhibition with minimal adverse metabolic consequences. This is particularly important as the PI3K/Akt/mTOR signaling pathway may be an important target in hyperinsulinemic women with breast cancer.

Materials and Methods

Animals

The mice used in this study were all on the FVB/N background. Wild type (WT) FVB/N mice and MKR mice that have been characterized previously were used (Fernandez *et al.* 2001, Novosyadlyy 2010). The mice were kept on a 12-h light/dark cycle, had free access to a standard mouse chow (Picolab rodent diet 5053; LabDiet, St. Louis, MO) and fresh water *ad libitum.* The Mount Sinai School of Medicine AAALAC accredited animal facility provided animal care and maintenance.

Orthotopic tumor models

Met-1 mammary tumor cells were initially derived from MMTV-PyVmT (FVB/N) transgenic mice (Borowsky *et al.* 2005) and MCNeuA mammary tumor cells were derived from MMTV-Neu (FVB/N) transgenic mice, the rodent equivalent of the human ERBB2 gene (Campbell *et al.* 2002). Cell culture, preparation and injection were performed as described previously (Novosyadlyy *et al.* 2010; Fierz *et al.* 2010). Tumor cells were inoculated into the 4th mammary fat pad of 8–10 week old female virgin homozygous MKR and WT FVB/N mice. Two weeks after Met-1 cell inoculation, tumors were matched according to size between groups, and mice were treated with either the pan-class I PI3K inhibitor NVP-BKM120 (50 mg/kg body weight per day by oral gavage), dissolved in 1-methyl-2-pyrrolidone NMP (Sigma-Aldrich, St Louis, MO, USA) and PEG 300 (Sigma-Aldrich, St Louis, MO, USA) to a ratio of 10% NMP: 90% PEG300, or the vehicle (10% NMP: 90% PEG 300). Similarly, treatment with the dual PI3K and mTOR inhibitor, NVP-BEZ235 (40mg tosylate salt/kg body weight per day by oral gavage) dissolved in NMP and mixed in PEG300 (10% NMP: 90% PEG300) or vehicle (10% NMP: 90% PEG300), began 2 weeks after Met-1 inoculation. Treatment continued in all groups for 14 days. Before and during treatment, tumor growth was measured in three dimensions (cranio-caudal, transverse and antero-posterior) using calipers. Tumor volume was calculated by the formula: $4/3 \times \pi \times r_1 \times r_2 \times r_3$ (r = radius). At the end of the study, mice were sacrificed and tumors were removed and weighed. NVP-BKM120 and NVP-BEZ235 were obtained free of charge through material transfer agreements with Novartis Pharma (Basel, Switzerland).

Protein extraction and Western blot analysis

Protein extraction and Western blot analysis was performed as previously described (Novosyadlyy et al 2010; Fierz *et al.* 2010). Phospho$^{(Ser\ 235/236)}$ and total S6 ribosomal protein, phospho$^{(Ser\ 473)}$ and total Akt, phospho$^{(Thr202/Tyr204)}$ and total p44/42 MAPK (Erk1/2) and Bcl-2 were purchased from Cell Signaling Technology (Danvers, MA, USA). The anti-β-actin antibody was purchased from Sigma Aldrich (St Louis, MO, USA).

Densitometric analysis was performed using ImageJ V1.44 software (National Institutes of Health, Bethesda, MD).

Immunofluorescence

To quantify 5-bromo-2-deoxyuridine (BrdU) incorporation (as detected by immunofluorescence), MKR and WT FVB/N mice were injected intraperitoneally with BrdU (Sigma Aldrich, St. Louis, MO) at 10 μl/gram of body weight, 2 h before sacrifice. Glands were fixed in 4% paraformaldehyde and embedded in paraffin. Sections were deparaffinized, rehydrated, and subjected to antigen retrieval as previously described (Cannata 2010). A mouse monoclonal antibody against BrdU (IIB5; 1:250; Santa Cruz Biotechnology, Santa Cruz, CA) was used. Immunofluorescence staining was detected by incubation with secondary AlexaFluor 488-conjugated (green) goat antimouse IgG (1:500; Molecular Probes) for 2 hours. Nuclei were counterstained with DAPI (0.2 μg/ml; Sigma Aldrich). At least twelve individual ×40 objective fields per group were captured for counting BrdU positive cells. The total number of DAPI positive cells and BrdU positive cells were counted and recorded. Results were expressed as the percent of BrdU / DAPI staining cells (Arpino 2007).

Metabolic assays

Blood glucose levels were checked weekly with an automated glucometer (Bayer Contour, IN, USA). Plasma insulin levels were measured by ELISA (Mercodia AB, Upsala, Sweden). A glucose tolerance test was performed after 8 h of fasting using a glucose bolus of 1.5 g/kg body weight administered by intraperitoneal injection. Blood glucose was measured from the tail vein immediately before (Time 0) and 15, 30, 60, and 120 minutes after glucose injection. Serum triglycerides were assayed by the triglycerides reagent set and manufacturers specifications (Pointe Scientific, Canton, MI, USA).

Statistical analysis

Results are expressed as the mean ± SEM. Statistical analyses were performed using the ANOVA followed by a Fisher's test. A p value of <0.05 was used to define statistical significance.

Acknowledgements

References

Agnoli C, Berrino F, Abagnato CA, Muti P, Panico S, Crosignani P, et al. Metabolic syndrome and postmenopausal breast cancer in the ORDET cohort: a nested case-control study. Nutr Metab Cardiovasc Dis. 2010; 20(1):41–48. [PubMed: 19361966]

Arpino G, Gutierrez C, Weiss H, Rimawi M, Massarweb S, Bharwani L, et al. Treatment of Human Epidermal Growth Factor Receptor 2-Overexpressing Breast Cancer Xenografts with Multiagent-Targeted Therapy. JNCI. 2007; 99(9):694–705. [PubMed: 17470737]

Borowsky AD, Namba R, Young LJ, Hunter KW, Hodgson JG, Tepper CG, et al. Syngeneic mouse mammary carcinoma cell lines: two closely related cell lines with divergent metastatic behavior. Clin Exp Metastasis. 2005; 22(1):47–59. [PubMed: 16132578]

Campbell MJ, Wollish WS, Lobo M, Esserman LJ. Epithelial and fibroblast cell lines derived from a spontaneous mammary carcinoma in a MMTV/neu transgenic mouse. In Vitro Cell Dev Biol Anim. 2002; 38(6):326–333. [PubMed: 12513120]

Cannata D, Lann D, Wu Y, Elis S, Sun H, Yakar S, Lazzarino D, Wood TL, LeRoith D. Elevated circulatory IGF-I promotes mammary gland development and proliferation. Endocrinology. 2010; 151(12):5751–5761. [PubMed: 20926579]

Creighton CJ, Fu X, Hennessy B, Casa AJ, Zhang Y, Gonzalez-Angulo AM, et al. Proteomic and transcriptomic profiling reveals a link between the PI3K pathway and lower estrogen receptor (ER) levels and activity in ER+ breast cancer. Breast Cancer Res. 2010; 12(3):R40. [PubMed: 20569503]

Fernandez AM, Kim JK, Yakar S, Dupont J, Hernandez-Sanchez C, Castle AL, Filmore J, Shulman GI, Le Roith D. Functional inactivation of the IGF-I and insulin receptors in skeletal muscle causes type 2 diabetes. Genes Dev. 2001; 15(15):1926–1934. [PubMed: 11485987]

Fierz Y, Novosyadlyy R, Vijayakumar A, Yakar S, LeRoith D. Mammalian target of rapamycin inhibition abrogates insulin-mediated mammary tumor progression in type 2 diabetes. Endocr Relat Cancer. 2010; 17(4):941–951. [PubMed: 20801951]

Foukas LC, Berejeno IM, Gray A, Khwaja A, Vanhaesebroeck B. Activity of any class 1A PI3K isoform can sustain cell proliferation and survival. Proc Natl Acad Science. 2010; 107:11381–11386.

Goodwin PJ, Ennis M, Pritchard KI, Trudeau ME, Koo J, Madarnas Y, et al. Fasting insulin and outcome in early-stage breast cancer: results of a prospective cohort study. J Clin Oncol. 2002; 20(1):42–51. [PubMed: 11773152]

Junttila TT, Akita RW, Parsons K, Fields C, Lewis Phillips GD, Friedman LS, et al. Ligand-independent HER2/HER3/PI3K complex is disrupted by trastuzumab and is effectively inhibited by the PI3K inhibitor GDC-0941. Cancer Cell. 2009; 15(5):429–440. [PubMed: 19411071]

Jia S, Liu Z, Zhang S, Liu P, Zhang L, Lee SH, Signoretti S, Loda M, Roberts TM, Zhao JJ. Essential roles of PI(3)K-p110beta in cell growth, metabolism and tumorigenesis. Nature. 2008; 454(7205): 776–779. [PubMed: 18594509]

Kohn AD, Summers SA, Birnbaum MJ, Roth RA. Expression of a constitutively active Akt Ser/Thr kinase in 3T3-L1 adipocytes stimulates glucose uptake and glucose transporter 4 translocation. J Biol Chem. 1996; 271(49):31372–31378. [PubMed: 8940145]

Liu LZ, Zhao HL, Zuo J, Ho SK, Chan JC, Meng Y, et al. Protein kinase Czeta mediates insulin-induced glucose transport through actin remodeling in L6 muscle cells. Mol Biol Cell. 2006; 17(5):2322–2330. [PubMed: 16525020]

López-Knowles E, O'Toole SA, McNeil CM, Millar EK, Qiu MR, Crea P, et al. PI3K pathway activation in breast cancer is associated with the basal-like phenotype and cancer-specific mortality. Int J Cancer. 2010; 126(5):1121–1131. [PubMed: 19685490]

Novosyadlyy R, Lann DE, Vijayakumar A, Rowzee A, Lazzarino DA, Fierz Y, et al. Insulin-mediated acceleration of breast cancer development and progression in a nonobese model of type 2 diabetes. Cancer Res. 2010; 70(2):741–751. [PubMed: 20068149]

O'Brien NA, Browne BC, Chow L, Wang Y, Ginther C, Arboleda J, et al. Activated phosphoinositide 3-kinase/AKT signaling confers resistance to trastuzumab but not lapatinib. Mol Cancer Ther. 2010; 9(6):1489–1502. [PubMed: 20501798]

Papa V, Pezzino V, Costantino A, Belfiore A, Giuffrida D, Frittitta L, et al. Elevated insulin receptor content in human breast cancer. J Clin Invest. 1990; 86(5):1503–1510. [PubMed: 2243127]

Patterson RE, Flatt SW, Saquib N, Rock CL, Caan BJ, Parker BA, et al. Medical comorbidities predict mortality in women with a history of early stage breast cancer. Breast Cancer Res Treat. 2010; 122(3):859–865. [PubMed: 20077000]

Peairs KS, Barone BB, Snyder CF, Yeh HC, Stein KB, Derr RL, et al. Diabetes mellitus and breast cancer outcomes: a systematic review and meta-analysis. J Clin Oncol. 2011; 29(1):40–46. [PubMed: 21115865]

Serra V, Markman B, Scaltriti M, Eichorn PJ, Valero V, Guzman M, et al. NVP-BEZ235, a dual PI3K/mTOR inhibitor,prevents PI3K signaling and inhibits the growth of cancer cells with activating PI3K mutations. Cancer Res. 2008; 68(19):8022–8030. [PubMed: 18829560]

Serra V, Scaltriti M, Prudkin L, Eichhorn PJ, Ibrahim YH, Chandarlapaty S, et al. PI3K inhibition results in enhanced HER signaling and acquired ERK dependency in HER2-overexpressing breast cancer. Oncogene. 2011; 30(22):2547–2557. [PubMed: 21278786]

Sopasakis VR, Liu P, Suzuki R, Kondo T, Winnay J, Tran TT, Asano T, Smyth G, Salan MP, Farese RV, Kahn CR, Zhao JJ. Specific roles of the p110alpha isoform of phosphatidylinositol 3-kinase in hepatic insulin signaling and metabolic regulation. Cell Metab. 2010; 11(3):220–230. [PubMed: 20197055]

Tan SX, Ng Y, James DE. Akt inhibitors reduce glucose uptake idependently of their effects on Akt. Biochem J. 2010; 432:191–197. [PubMed: 20819080]

Um SH, D'Alessio D, Thoma G. Nutrient overload, insulin resistance and ribosomal protein S6 kinase 1, S6K1. Cell Metab. 2006; 3(6):393–402. [PubMed: 16753575]

Wells V, Downward J, Malluci L. Functional inhibition of PI3K by the betaGBP molecule suppresses Ras-MAPK signaling to block cell proliferation. Oncogene. 2007; 26:7709–7714. [PubMed: 17603562]
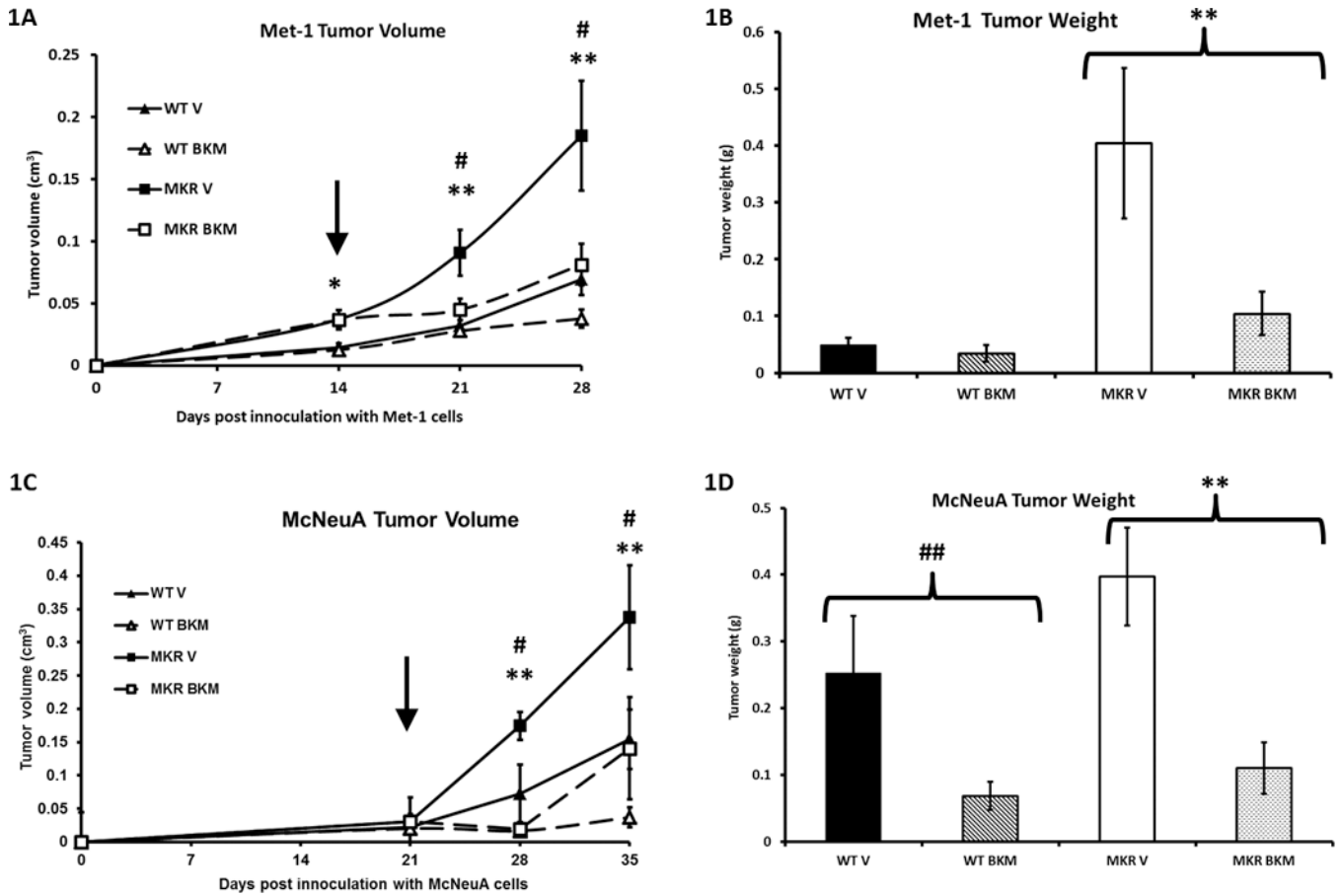
Figure 1.
Treatment with NVP-BKM120 reduced the accelerated tumor growth in the MKR mice. 1A and 1C: Met-1 cells (0.5×10^6) and MCNeuA cells (1×10^6) were injected into the 4th mammary fat pad of 8–10 week old virgin wild-type (WT) and MKR mice on day 0. Treatment with NVP-BKM120 (BKM) or vehicle (V) began 2 weeks after Met-1 cell injection and 3 weeks after MCNeuA cell injection (arrows). Tumor volume was measured during the 2 weeks of treatment with NVP-BKM120 or vehicle. 1B, 1D: Tumor weight was measured at necropsy. All data are expressed as mean ± SEM. * P<0.05 between WT and MKR groups. ** P<0.05 between MKR NVP-BKM120 and MKR vehicle groups. # P<0.05 between MKR vehicle group and WT vehicle group. ## P<0.05 between WT NVP-BKM120 and WT vehicle treated group. n=8–9 mice / group.
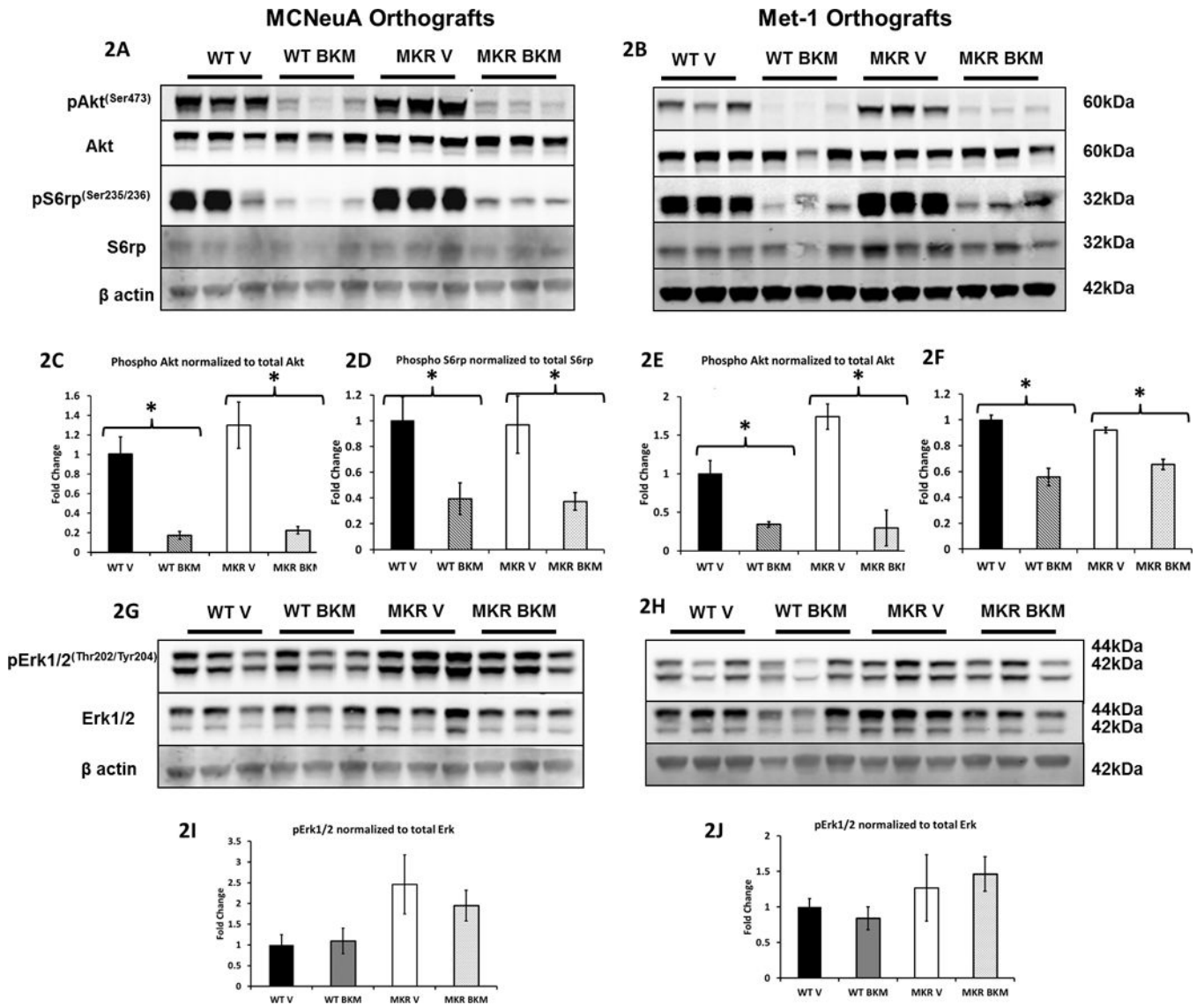
Figure 2.

Treatment with NVP-BKM120 reduced serine phosphorylation of Akt and S6 ribosomal protein in MCNeuA and Met-1 tumors treated with NVP- BKM120. Protein extracts from MCNeuA and Met-1 tumors from WT and MKR mice were size fractionated and immunoblotted against phospho(Ser 473) and total Akt, phospho(Ser 235/236) and total S6 ribosomal protein, phospho(Thr202/Tyr204)and total Erk1/2 (2A, 2B, 2G, 2H). Representative western blot analyses are displayed for MCNeuA tumors (2A and 2G) and Met-1 tumors (2B and 2H). Figures 2C–2F, 2I, 2J display the densitometric analyses of phosphorylated Akt normalized to total Akt, phosphorylated S6rp normalized to total S6rp levels, and phosphorylated Erk1/2 normalized to total Erk1/2, for MCNeuA and Met-1 tumors. Data in 2C–2F, 2I, 2J are presented as a fold change in the mean (±SEM) of each group compared to the WT vehicle treated group. * P<0.05 between groups. Statistically significant increases in Akt phosphorylation normalized to total Akt in MCNeuA and Met-1 tumors rom the MKR
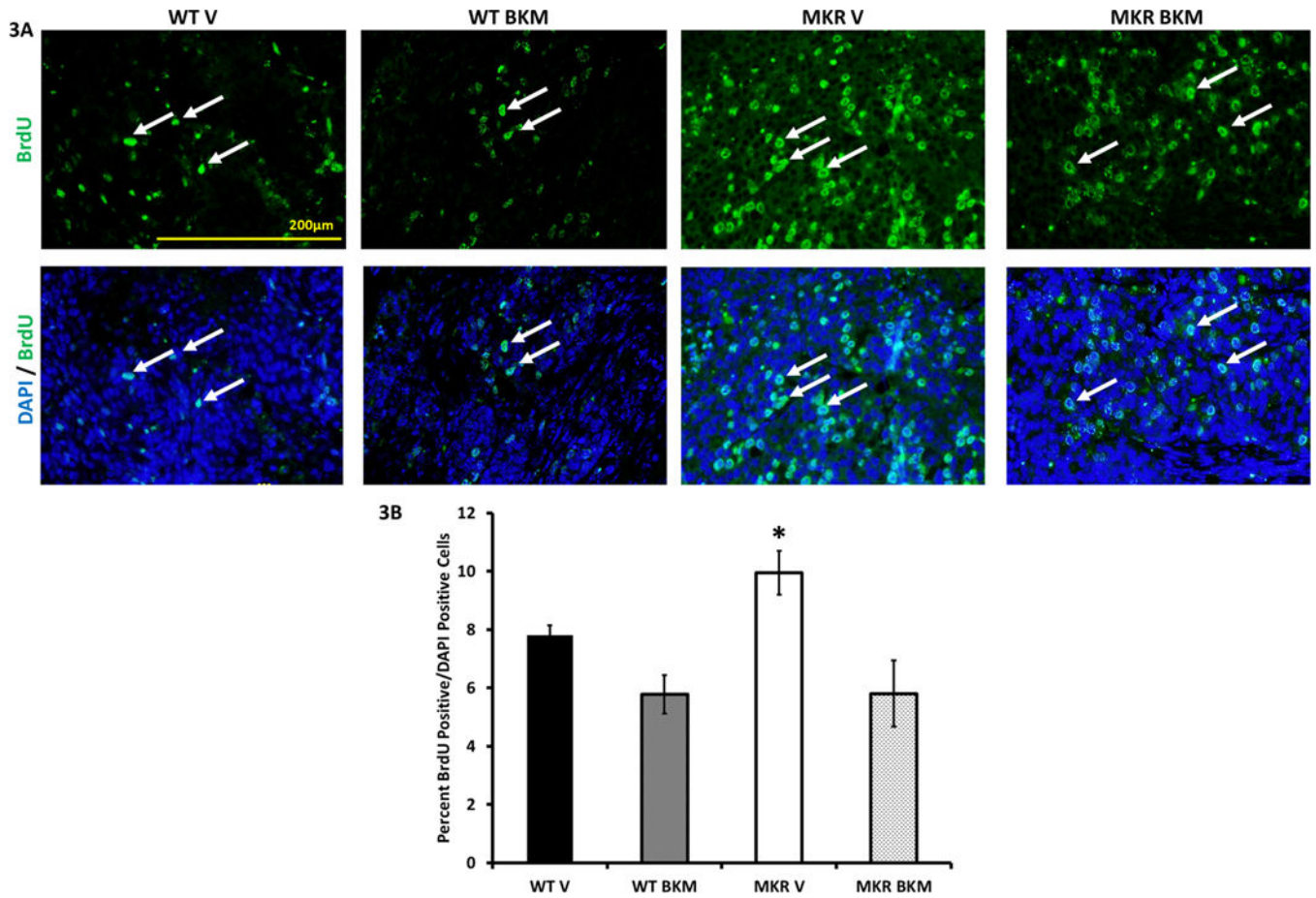
V mice compared to the WT V mice (not marked with asterisk in Fig 2C and 2E). (WT = wild type, V = vehicle treated, BKM = NVP-BKM120 treated).
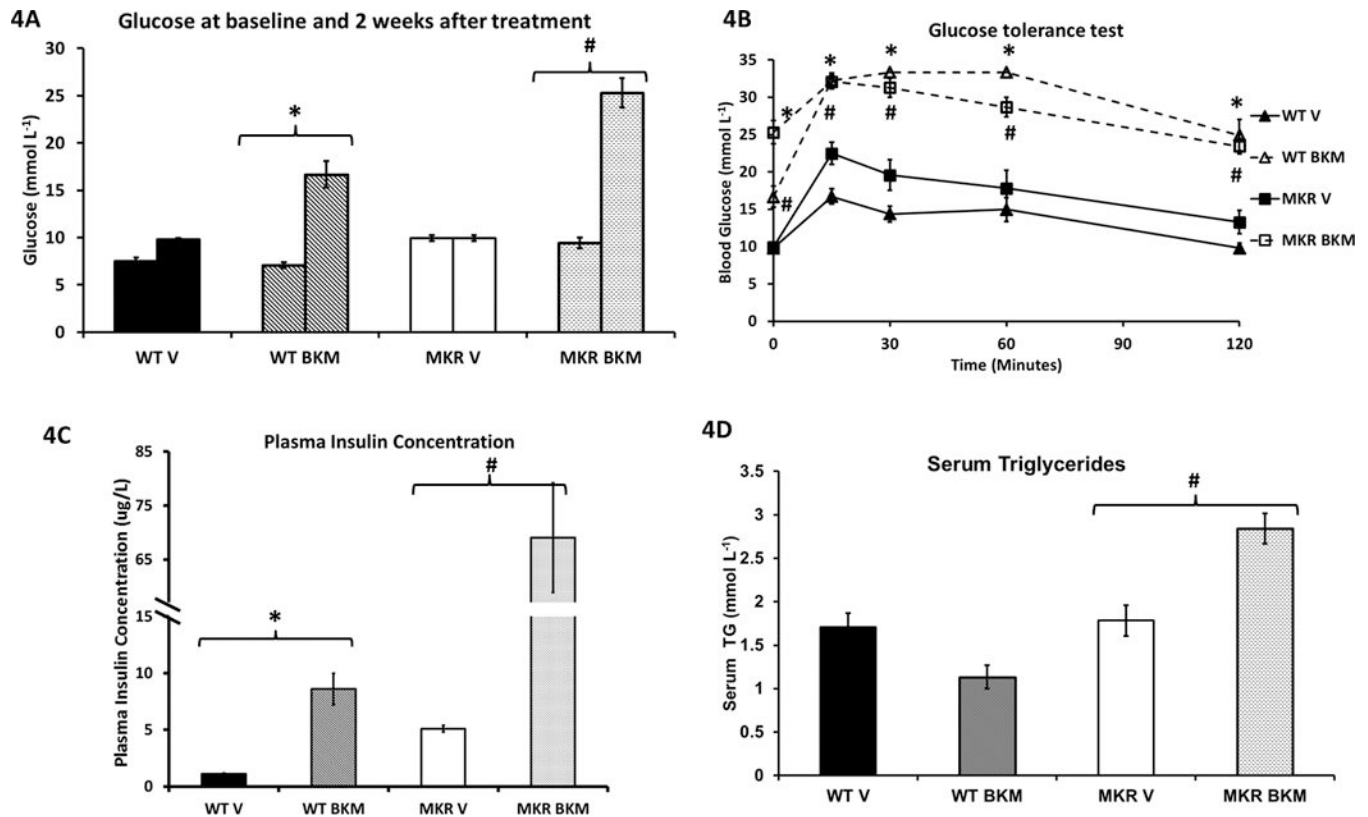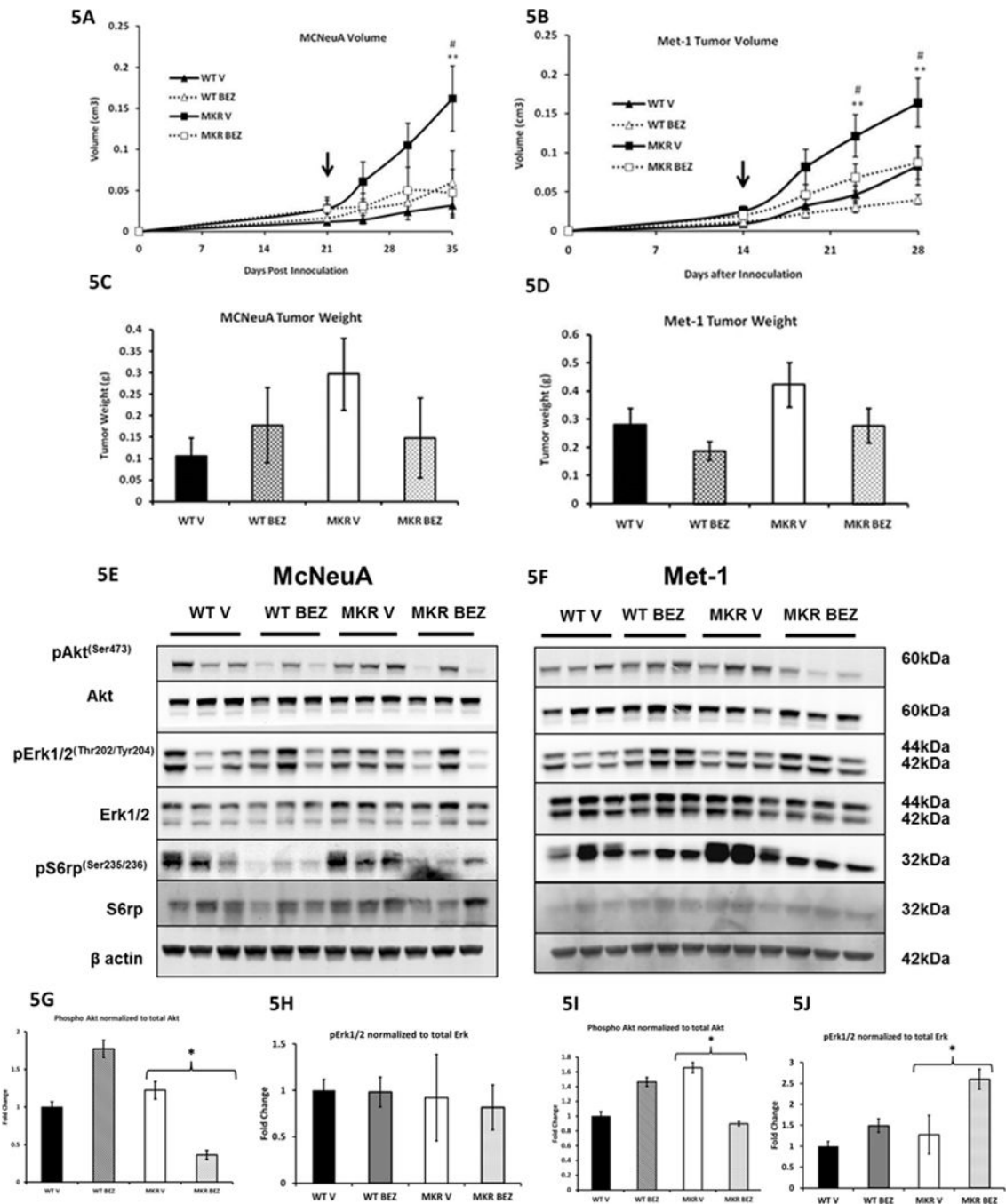
Figure 3.
NVP-BKM120 reduces the increased proliferation of Met-1 cell orthografts in MKR mice. Assessment of proliferation of Met-1 orthografts by BrdU incorporation, after intraperitoneal injection of BrdU (10μl/g body weight) and detection by immunofluorescence (mouse monoclonal antibody against BrdU, secondary antibody AlexaFluor 488-conjugated goat antimouse IgG (green), and nuclear counterstaining with DAPI (blue). 3A: Representative 40X objective images of BrdU positive Met-1 tumors (top row) and composite images of DAPI and BrdU positive Met-1 tumors (bottom row). White arrows point to BrdU positive cells. 3B: Quantitative analysis representing the percent of BrdU positive cells to total number of DAPI positive cells, expressed as means ± SEM. *$P < 0.05$ between MKR vehicle treated group and all other groups (n = 2–3 mice per group, with six 40X fields per mouse). (WT = wild type, V = vehicle treated, BKM = NVP-BKM120 treated).

Figure 4.

NVP-BKM120 treatment led to hyperglycemia, hypertriglyceridemia and exacerbated hyperinsulinemia in MKR mice. 4A: Mean random glucose levels at start of treatment with NVP-BKM120 or vehicle and after 2 weeks of treatment. 4B: Results of the 1.5g/kg glucose tolerance test. Glucose was injected at time 0 and glucose measurements were taken at 0, 15, 30, 60 and 120 minutes. 4C. Plasma insulin concentrations of the WT and MKR mice after 2 weeks of treatment with NVP-BKM120 or vehicle. The y-axis is broken at the parallel lines and the bar for the MKR BKM group is broken at the same point to aid visualization of the WT groups. 4D. Serum Triglyceride (TG) concentration in WT and MKR mice after 2 weeks of treatment with NVP-BKM120 or vehicle. All data are presented as the mean ±SEM, *P<0.05 between the WT NVP-BKM120 treated mice and WT vehicle group. # P<0.05 between MKR NVP-BKM120 treated mice and MKR vehicle treated group. (WT = wild type, V = vehicle treated, BKM = NVP-BKM120 treated).

Figure 5.

NVP-BEZ235 treatment reduced tumor volume in the MKR treated group, and decreased Akt[Ser 473] and S6rp [Ser 235/236] phosphorylation.5A–5B: MCNeuA cells and Met-1 cells were injected into the 4th mammary fat pad as outlined in the methods section and Figure 1. NVP-BEZ235 (BEZ) and vehicle (V) treatment began 2 weeks after Met-1 injection and 3 weeks after MCNeuA injection (arrows). 5A and 5B: Tumor volumes were measured during the 2 weeks of treatment. # P 0.05 between MKR NVP-BEZ235 and vehicle treated groups. ** P<0.05 between MKR NVP-BKM120 and MKR vehicle groups. # P<0.05 between MKR

vehicle group and WT vehicle group. ## P<0.05 between WT NVP-BKM120 and WT vehicle treated group. Figure 5C, 5D: Tumor weight was measured at the end of the study. Figure 5E–F: Representative western blots demonstrating protein extracts from MCNeuA and Met-1 tumors from WT and MKR mice treated with vehicle (V) and NVP-BEZ235 (BEZ). 5G–5I: Densitometric analysis for MCNeuA and Met-1 tumors of the relative phosphorylation of Akt to total Akt and phosphorylation of Erk1/2 to total Erk1/2. Results are displayed as mean±SEM and are presented as a fold change compared to the WT vehicle treated group. *P<0.05 between groups.
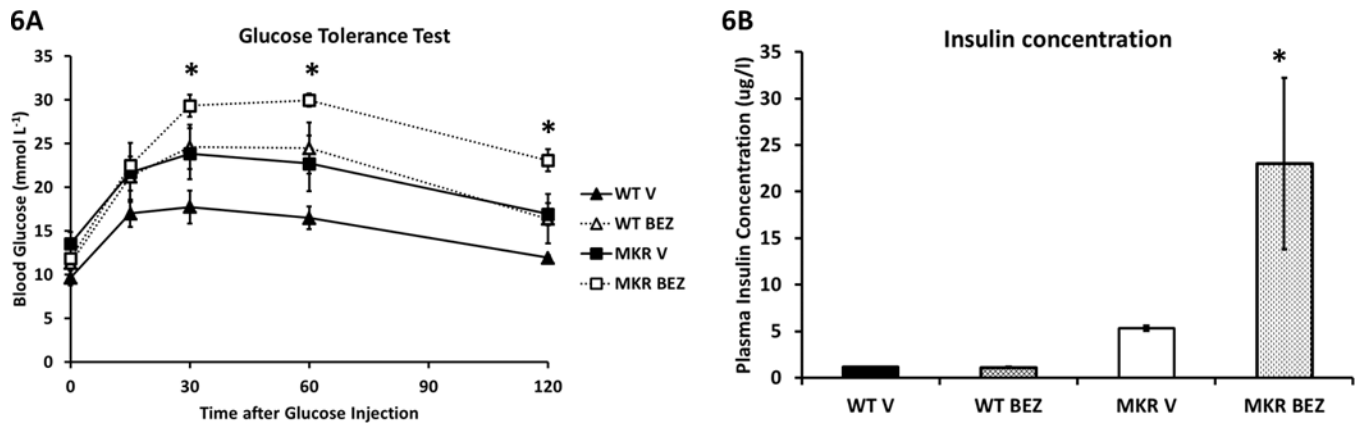
Figure 6.
Metabolic investigations demonstrated worsening glucose tolerance and hyperinsulinemia in the MKR mice treated with NVP-BEZ235. 6A: Results of the 1.5g/kg glucose tolerance test. Glucose was injected at time 0 and glucose measurements were taken at 0, 15, 30, 60 and 120 minutes. * $P<0.05$ between glucose levels of the MKR NVP-BEZ235 treated mice compared to MKR vehicle treated group. 6B:. Plasma insulin concentrations of the WT and MKR mice after 2 weeks of treatment with NVP-BEZ235 or vehicle. *$P<0.05$ between the MKR NVP-BEZ235 treated mice and MKR vehicle treated group and WT groups..Results are expressed as mean±SEM,. (WT = wild type, V = vehicle treated, BEZ = NVP-BEZ235 treated).